THE JOURNAL OF BIOLOGICAL CHEMISTRY VOL. 283, NO. 6, pp. 3392–3400, February 8, 2008
© 2008 by The American Society for Biochemistry and Molecular Biology, Inc. Printed in the U.S.A.

NF-κB-inducing Kinase Phosphorylates and Blocks the Degradation of Down Syndrome Candidate Region 1*

Received for publication, August 13, 2007, and in revised form, November 29, 2007 Published, JBC Papers in Press, December 4, 2007, DOI 10.1074/jbc.M706707200

Eun Jung Lee[‡], Su Ryeon Seo[§], Ji Won Um[‡], Joongkyu Park[‡], Yohan Oh[‡], and Kwang Chul Chung[‡1]

From the [‡]Department of Biology, College of Science, Yonsei University, Seoul 120-749 and the [§]Department of Molecular Bioscience, School of Bioscience and Biotechnology, Kangwon National University, Chuncheon, Kangwon-do 200-701, Korea

Down syndrome, the most frequent genetic disorder, is characterized by an extra copy of all or part of chromosome 21. Down syndrome candidate region 1 (DSCR1) gene, which is located on chromosome 21, is highly expressed in the brain of Down syndrome patients. Although its cellular function remains unknown, DSCR1 expression is linked to inflammation, angiogenesis, and cardiac development. To explore the functional role of DSCR1 and the regulation of its expression, we searched for novel DSCR1-interacting proteins using a yeast two-hybrid assay. Using a human fetal brain library, we found that DSCR1 interacts with NF-κB-inducing kinase (NIK). Furthermore, we demonstrate that NIK specifically interacts with and phosphorylates the C-terminal region of DSCR1 in immortalized hippocampal cells as well as in primary cortical neurons. This NIK-mediated phosphorylation of DSCR1 increases its protein stability and blocks its proteasomal degradation, the effects of which lead to an increase in soluble and insoluble DSCR1 levels. We show that an increase in insoluble DSCR1 levels results in the formation of cytosolic aggregates. Interestingly, we found that whereas the formation of these inclusions does not significantly alter the viability of neuronal cells, the overexpression of DSCR1 without the formation of aggregates is cytotoxic.

Down syndrome (DS),[2] the most common genetic disorder, occurs in one of every 700–800 births. Patients with DS display many typical phenotypes, such as immune deficiency, characteristic facial features, mental retardation, congenital heart disease, and early onset Alzheimer disease-like symptoms (1, 2). DS is associated with having three copies of chromosome 21, also known as trisomy 21 (3, 4), and the overexpression of a number of genes located on this chromosome is thought either directly or indirectly to be responsible for these clinical features.

Down syndrome candidate region 1 (DSCR1, also called as Adapt78, MCIP1, calcipressin 1, or RCAN1) gene is located near the Down syndrome critical region of chromosome 21 (5, 6). It is highly expressed in the brain, heart, and skeletal muscles of DS fetuses (7), and it is known to interact physically and functionally with Ca^{2+}/calmodulin-dependent protein phosphatase 2B (also known as calcineurin A; see Ref. 8). DSCR1 has been proposed to be a feedback inhibitor of calcineurin based on two controversial findings. First, the overexpression of DSCR1 suppresses calcineurin signaling, and second, calcineurin activity in the hearts of DSCR1 knock-out mice is greatly diminished (9, 10). Moreover, the proper expression of DSCR1 appears to be linked to inflammation, angiogenesis, and cardiac development (11–14).

NF-κB-inducing kinase (NIK), a Ser/Thr kinase, is a member of mitogen-activated protein kinase (MAPK) kinase kinase family. It preferentially phosphorylates and therefore activates IκB kinase α (IKKα) (15, 16). NIK and IKKα are known to induce the processing of p100 and the generation of p52, thereby activating the alternative NF-κB pathway (17). Although the physiological role of NIK in NF-κB signaling is unclear, gene knock-out studies have suggested that NIK regulates the transcriptional activity of NF-κB in a receptor-restricted manner, such as by both tumor necrosis factor-α and interleukin-1β (18). $NIK^{-/-}$ cells are also unable to induce NF-κB-dependent gene transcription in response to treatment with lymphotoxin-β despite IκBα degradation (18). NIK has both functional nuclear import and export signals that result in its continuous shuttling between the cytoplasm and the nucleus, which suggests that NIK, like IKKα, has an intranuclear function (19).

The nuclear factors of activated T cells (NF-ATs) are a family of transcription factors that transduce calcium signals in the immune, cardiac, muscular, and nervous systems (20). Like their distant relatives the Rel family, which includes NF-κB, NF-ATs are located in the cytoplasm of resting cells and are activated by their induced nuclear import (21). Calcium signaling activates calcineurin and induces the movement of NF-AT proteins into the nucleus, where they cooperate with other proteins to form complexes on DNA. Some NF-ATs are characterized by a highly conserved DNA-binding domain as well as a

* This work was supported by Grants from the Brain Research Center of the 21st Century Frontier Research Program Technology M103KV010011-06K2201-01110 (to K. C. C.), from National Research Laboratory Program Grant R04-2007-000-20014-0 (to K. C. C.) of Korea Science and Engineering Foundation (KOSEF) funded by Ministry of Science, Republic of Korea, and in part by Basic Research Grant from KOSEF R01-2007-000-20089-0 (to K. C. C.), by Grant A060440from the Korea Health 21 R & D Project (to K. C. C.), Ministry of Health & Welfare, and by the Korea Research Foundation Grant KRF-2004-005-E0017 (to K. C. C. and S. R. S.). The costs of publication of this article were defrayed in part by the payment of page charges. This article must therefore be hereby marked "*advertisement*" in accordance with 18 U.S.C. Section 1734 solely to indicate this fact.

[1] To whom correspondence should be addressed: Dept. of Biology, College of Science, Yonsei University, Shinchon-dong 134, Seodaemun-gu, Seoul 120-749, Korea. Tel.: 82-2-2123-2653; Fax: 82-2-312-5657; E-mail: kchung@yonsei.ac.kr.

[2] The abbreviations used are: DS, Down syndrome; DSCR1, Down syndrome candidate region 1; HEK293, human embryonic kidney 293; IKKα, IκB kinase α; MTT, 3,(4,5-dimethyldiazol-2-yl)2,5-diphenyl-tetrazolium bromide; NF-ATs, The nuclear factors of activated T cells; NIK, NF-κB-inducing kinase; PBS, phosphate-buffered saline; HA, hemagglutinin; GFP, green fluorescent protein; GST, glutathione *S*-transferase; TUNEL, terminal dUTP nick-end labeling.

This is an Open Access article under the CC BY license.

calcineurin-binding domain (22). The binding of calcineurin to the latter domain controls the nuclear transport of these NF-ATs (22). Although many reports have suggested a physiological link between the NF-κB and NF-AT pathways, the functional linkage between these two signaling pathways has yet to be determined.

In the study presented here, we investigated the cellular function of DSCR1 by searching for novel binding partner(s). We found that NIK selectively binds to and phosphorylates the C-terminal region of DSCR1. Furthermore, we demonstrate that this phosphorylation of DSCR1 enhances its stability, which in turn leads to an increase in the levels of soluble and insoluble DSCR1.

EXPERIMENTAL PROCEDURES

Materials—The following materials were used. Synthetic dropout medium (SD/T, SD/L, and SD/HLT) and yeast extract peptone dextrose medium containing adenine were purchased from MP Biomedicals (Solon, OH). The human fetal brain cDNA library was purchased from Clontech. Peroxidase-conjugated anti-rabbit and anti-mouse IgGs were purchased from Zymed Laboratories Inc.. All cell culture reagents, including Dulbecco's modified Eagle's medium and fetal bovine serum, and TRIzol reagent were purchased from Invitrogen. Protein A-Sepharose was purchased from Amersham Biosciences, and enhanced chemiluminescence reagents and [γ-^{32}P]ATP were purchased from PerkinElmer Life Sciences. Polyclonal and monoclonal anti-HA, anti-GFP, and anti-NIK antibodies were from Santa Cruz Biotechnology (Santa Cruz, CA) and anti-FLAG antibody and cycloheximide were purchased from Sigma. Clasto-lactacystin β-lactone and MG132 were purchased from Calbiochem. A mammalian expression vector for HA-tagged human wild type DSCR1 was kindly provided by S. de la Luna (Genomics Regulation Center, Barcelona, Spain), and plasmids encoding wild type and deletions of GFP-tagged DSCR1 and HA-tagged wild type calcineurin A were kindly provided by B. A. Rothermel (University of Texas Southwestern Medical Center, Dallas). GST-tagged bacterial expression vectors encoding amino acids 1–197 (full length), 1–90, and 90–197 of DSCR1 were constructed by subcloning PCR products from HA-tagged DSCR1 into pGEX-4T1 (Amersham Biosciences) and confirmed by DNA sequencing. Mammalian expression vectors for Myc-tagged wild type NIK and its kinase-deficient mutants, such as Myc-NIK-KD (in which the catalytic domain of NIK from amino acids 100–250 is deleted) and Myc-NIK-KKAA (in which lysine residues at position 429 and 430 are mutated to alanine), were gifts from T. H. Lee (Yonsei University, Seoul, Korea). Rabbit polyclonal antibody of DSCR1 was produced commercially (Lab Frontier, Seoul, Korea) by injecting purified GST-DSCR1. The serum from these rabbits was then affinity-purified using standard methods.

Yeast Two-hybrid Assay—Screening was performed using a 13-week human fetal brain Matchmaker cDNA library subcloned into the activation domain of pACT2 vector, and yeast strain carrying the pHybTrp/Zeo-plasmid that encoded for wild type DSCR1 was used as bait. The yeast strain L40, which contains the reporter genes *lacZ* and *HIS3* under the control of *LexA* promoter, was sequentially transformed with bait vector then the cDNA library vectors, and the cells were plated on a synthetic medium containing 5 mM 3-amino-1,2,4-triazole and lacking histidine, leucine, and tryptophan. After 10–14 days at 30 °C, the transformants were grown on synthetic medium containing 50 μg/ml of 5-bromo-4-chloro-3-indolyl-D-galactoside, but lacking histidine, leucine, and tryptophan. After 2–3 days at 30 °C, the resulting yeast colonies displaying a blue color were selected as positive clones. The plasmids from these positive clones were extracted in lysis buffer containing 2% Triton X-100, 1% SDS, 100 mM NaCl, 10 mM Tris, pH 8.0, and 1.0 mM EDTA and then transformed into *Escherichia coli* DH5α by electroporation. The inserts of the plasmids from the positive library clones were analyzed using an automatic DNA sequencer (ALF Express, Amersham Biosciences).

Cell Culture—Human embryonic kidney 293 (HEK293) cells and rat embryonic hippocampal (H19-7) cells were maintained in Dulbecco's modified Eagle's medium supplemented with 10% fetal bovine serum, penicillin, and streptomycin. These cells were transfected with the Lipofectamine plus reagent (Invitrogen) using the supplier's recommended instructions. To prepare lysates, the cells were rinsed twice with ice-cold phosphate-buffered saline (PBS), solubilized in lysis buffer (Tris, pH 7.9, containing 1.0% Nonidet P-40, 150 mM NaCl, 1 mM EGTA, 1 mM EDTA, 10% glycerol, 1 mM Na_3VO_4, 1 μg/ml leupeptin, 1 μg/ml aprotinin, 10 mM NaF, and 0.2 mM phenylmethylsulfonyl fluoride), and then scraped. Supernatant was collected after centrifugation for 10 min at 14,000 $\times$ *g* at 4 °C. Protein concentrations were determined using the Bio-Rad detergent-compatible protein assay kit according to the manufacturer's instructions.

Immunoprecipitation and Western Blot Analysis—One microgram of antibody was incubated with 2 mg of cell extracts in lysis buffer overnight at 4 °C. Fifty microliters of a 1:1 suspension of protein A-Sepharose beads were added, and the mixture was incubated for 2 h at 4 °C with gentle rotation. The beads were pelleted and washed extensively with cell lysis buffer. Bound proteins were dissociated by boiling in SDS-PAGE sample buffer, and whole protein samples were separated on an SDS-polyacrylamide gel and then transferred to a nitrocellulose membrane (Millipore, Japan). The membranes were blocked in TBST buffer (20 mM Tris, pH 7.6, 137 mM NaCl, 0.05% Tween 20, and 3% nonfat dried milk) for 3 h and then incubated overnight at 4 °C in 3% nonfat dried milk containing the appropriate antibodies. The membranes were washed several times in TBST and then incubated with IgG-coupled horseradish peroxidase secondary antibody (Zymed Laboratories Inc.). After 60 min, the blots were washed several times with TBST, and resulting immunocomplexes were visualized using enhanced chemiluminescence according to the manufacturer's instructions.

Reverse Transcription-PCR—Total cellular mRNA was extracted using the TRIzol reagent. cDNA was synthesized by reverse transcription using random primers. Two micrograms of cDNA were used per PCR. The primers used were as follows: rat *dscr1* forward, 5′-C CGGAATTCATGCATTTTAGGGACTTTA-3′, and rat *dscr1* reverse, 5′-CCGCTCAAGGCTGAGGTGGATGGG-3′; human *dscr1* forward, 5′-GAGGAG-

GTGGACCTGCAGGACCTG-3′, and human *dscr1* reverse, 5′-TCAGCTGAGGTGGATCGGCGTGTAC-3′.

Preparation of Nonidet P-40-soluble/insoluble Fractions—Cells were solubilized with 1.0% Nonidet P-40, and the resulting cellular suspension was fractionated by centrifugation at 15,000 × *g* for 30 min. The supernatants (*i.e.* the Nonidet P-40-soluble fraction) were directly immunoprecipitated. The resulting pellet (*i.e.* the Nonidet P-40-insoluble fraction) was washed three times with ice-cold lysis buffer and then solubilized in 4% SDS sample buffer (0.5 M Tris-HCl, pH 6.8, 20% glycerol, 4% SDS, 10% mercaptoethanol) for 1 h at 60 °C.

Immunocytochemistry—Cells were seeded overnight at 70% confluence onto coverslips in 6-well dishes. The following day, the cells were transfected. Twenty four hours later, the cells were washed with PBS, fixed with neutrally buffered 4% (w/v) paraformaldehyde, and permeabilized with 1% PBS solution containing 0.1% Triton X-100 for 1 h. The cells were then incubated for 24 h at 4 °C with the indicated primary antibody diluted in PBS containing 1% bovine serum albumin. After washing three times with PBS, the cells were incubated with secondary antibody for 2 h at room temperature. The cells were then analyzed using either fluorescence (IX71, Olympus) or confocal microscopy (LSM 510 META, Carl Zeiss).

Preparation of Cytosolic and Nuclear Fractions—Cells were washed with ice-cold PBS, resuspended in hypotonic buffer (10 mM HEPES, pH 7.9, 1.5 mM $MgCl_2$, 10 mM KCl) supplemented with protease inhibitors (dithiothreitol, aprotinin, and leupeptin), and then incubated on ice for 30 min. The cells were then lysed using a disposable syringe, and the lysates were subjected to centrifugation at 3,000 rpm for 15 min at 4 °C. The resulting supernatant was used as the cytosolic fraction. The resulting pellet, which was used as the nuclear fraction, was washed with hypotonic buffer and lysed with 1.0% Nonidet P-40 lysis buffer. Supernatants from each fraction were collected after centrifugation at 14,000 × *g* for 10 min at 4 °C.

In Vitro Kinase Assay—Confluent cells were harvested using lysis buffer. The soluble lysates were incubated with the indicated antibodies for 2 h at 4 °C. Following the addition of protein A-Sepharose beads, the mixture was incubated for 2 h at 4 °C and then rinsed with lysis and kinase buffers. Immunocomplex kinase assays were performed by incubating the cell lysates with the substrate in the reaction buffer (0.2 mM sodium orthovanadate, 2 mM dithiothreitol, 10 mM $MgCl_2$, 5 mCi of [γ-^{32}P]ATP, 100 μM ATP, and 20 mM HEPES, pH 7.4) for 2 h at 30 °C. The reactions were terminated, and the mixtures were subject to SDS-PAGE. Phosphorylated substrates were visualized by autoradiography.

Assessment of Cell Survival (MTT Extraction Assay)—3,(4,5-Dimethyldiazol-2-yl)2,5-diphenyl-tetrazolium bromide (MTT, 62.5 μl of a 5 mg/ml stock solution) was added to the 250 μl of medium in each well of a 24-well plate. After a 2-h incubation at 37 °C, 250 μl of extraction buffer (20% SDS and 50% *N*,*N*-dimethylformamide, pH 7.4) was added. After an overnight incubation at 37 °C, the absorbance at 570 nm was measured using a VERSA MAX enzyme-linked immunosorbent assay reader (Molecular Devices, Sunnyvale, CA) with an extraction buffer negative control.

TUNEL Assay—Cells were seeded overnight at 70% confluence onto coverslips in 6-well dishes. The following day, the cells were transfected with the indicated plasmids, incubated for 24 h, and then treated with zinc for 1 h. Cell apoptosis was analyzed using an *in situ* cell death detection kit (TMR red, Roche Applied Science) that is based on the terminal TUNEL technology.

RESULTS

Identification of Novel DSCR1-interacting Proteins Using a Yeast Two-hybrid Assay—To identify novel DSCR1-interacting partners, a yeast two-hybrid assay was performed using a human fetal brain cDNA library with full-length DSCR1 as the bait. We found several previously identified DSCR1-interacting proteins, such as calcineurin A (8) and Raf-1 (23), which indicates that the assay is a reliable method for identifying DSCR1-interacting proteins. In addition to the known DSCR1-interacting proteins, our assay identified NIK as a protein that interacts with DSCR1 (data not shown). Based on the known physiological substrate of NIK and the fact that DSCR1 function is regulated by its protein stability, which in turn is affected by its phosphorylation status, the functional connection between DSCR1 and NIK was further characterized.

DSCR1 Interacts with NIK in Neuronal Cells—Using an immunoprecipitation binding assay, we examined the potential interaction of NIK and DSCR1 in mammalian neuronal cells. H19-7 cells were transiently transfected with HA-tagged human wild type DSCR1 alone, or in the presence of Myc-tagged NIK. Extracts from the transfected cells were then subjected to immunoprecipitation using either anti-HA or anti-Myc antibodies and then immunoblot analysis using anti-Myc or anti-HA antibodies (Fig. 1*A*). This analysis revealed that DSCR1 associated with NIK (Fig. 1*A*). The use of preimmune IgG and empty protein A beads as negative controls (Fig. 1*A*) demonstrates that transiently transfected DSCR1 selectively binds to NIK in H19-7 cells. Next we examined whether IKKα, the only known substrate of NIK, also associates with DSCR1. Cells were transfected with HA-tagged IKKα and/or GFP-tagged DSCR1 and then subjected to immunoprecipitation. The results demonstrate that IKKα does not interact with DSCR1 (Fig. 1*B*). HA-tagged calcineurin A was used as a positive control in the GFP-tagged DSCR1 binding assay in H19-7 cells to demonstrate the reliability of the co-immunoprecipitation assay (Fig. 1*C*).

To determine whether DSCR1 and NIK interact in the absence of exogenous DNA addition, we examined the specific binding of endogenous DSCR1 and NIK in primary neuronal cells and transformed H19-7 cell line using co-immunoprecipitation assays. As shown in Fig. 2, *A* and *B*, we found that endogenous NIK binds to endogenous DSCR1 in both H19-7 cells and primary cortical neurons. Immunoprecipitation using nonspecific IgG was used as a negative control. This interaction was also observed in rat whole brain lysates (Fig. 2*C*), suggesting that the specific interaction between DSCR1 and NIK is not an artifact of DNA transfection and transformation but actually occurs in the mammalian central nervous system.

Wild Type NIK Binds to the C-terminal Domain of DSCR1—To determine the protein domain(s) responsible for the inter-

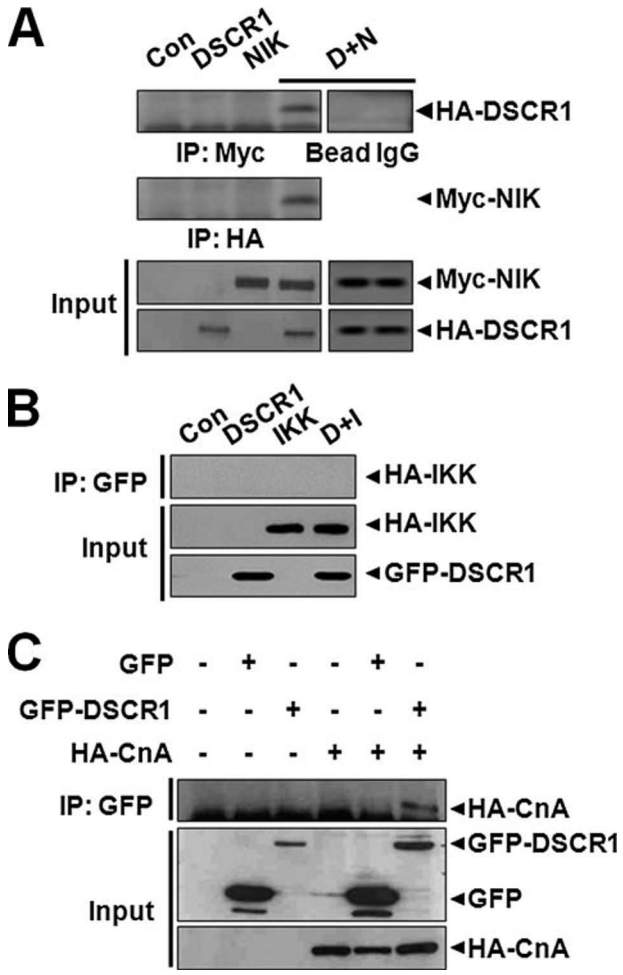

FIGURE 1. **DSCR1 specifically binds to NIK in H19-7 cells.** *A,* H19-7 cells were either mock-transfected (*Con*) or transiently transfected with 2 μg of HA-DSCR1 (*DSCR1* or *D*) and/or 2 μg of Myc-NIK (*NIK* or *N*), as indicated. Total cell lysates were immunoprecipitated (*IP*) with anti-HA or anti-Myc antibodies followed by Western blot analysis with anti-HA or -Myc antibodies. The levels of exogenous Myc-NIK and HA-DSCR1 proteins were examined with their respective epitope-specific antibodies. Where indicated, the cells were transfected with Myc-NIK and HA-DSCR1, and the cell lysates were immunoprecipitated with either preimmune IgG (*IgG*) or empty protein A-beads (*Bead*). The immunoprecipitates were examined by Western blot analysis with anti-HA antibodies. *B,* H19-7 cells were mock-transfected (*Con*) or transfected with HA-tagged IKKα (*IKK* or *I*) and/or GFP-tagged DSCR1 (*DSCR1* or *D*). Twenty four hours later, lysates from the cells were immunoprecipitated with anti-GFP antibodies followed by Western blot analysis with anti-HA antibodies. The expression of HA-tagged IKKα and GFP-tagged DSCR1 in the cell lysates was examined by Western blotting with either anti-HA or anti-GFP IgGs as indicated. *C,* H19-7 cells were mock-transfected or transfected with GFP, GFP-tagged DSCR1, and/or HA-tagged calcineurin A (*CnA*). Twenty four hours later, lysates from these cells were IP with anti-GFP antibodies followed by Western blotting with anti-HA antibodies. The expression of exogenous GFP, GFP-tagged DSCR1, and HA-tagged calcineurin in the cell lysates was confirmed by immunoblotting with either anti-GFP or anti-HA IgGs, as indicated.

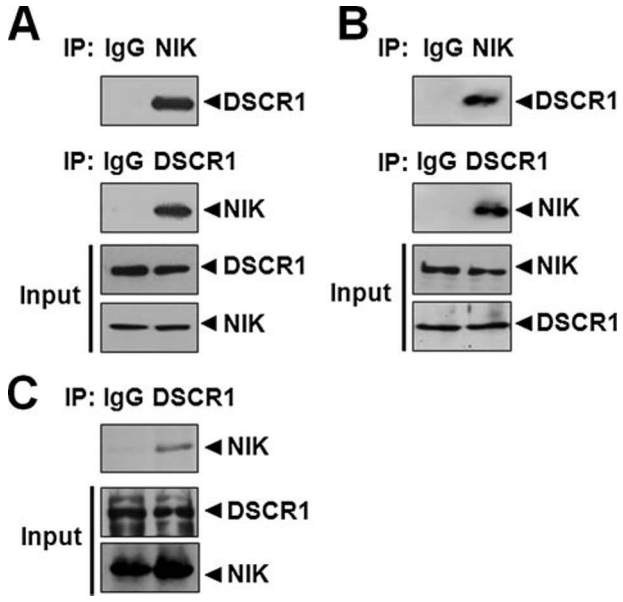

FIGURE 2. **Endogenous DSCR1 binds to NIK in rat primary neurons.** Cell extracts prepared from H19-7 cells (*A*) or rat primary cortical neurons (*B*) were immunoprecipitated (*IP*) with anti-NIK or anti-DSCR1 antibodies, as indicated. The immunocomplexes were analyzed by Western blotting with anti-DSCR1 and anti-NIK antibody. The endogenous levels of the proteins in the cell lysates were examined by immunoblot analysis, as indicated. *C,* whole cell lysates from rat brain were prepared with gentle homogenization, and immunoprecipitation was performed on these lysates with anti-DSCR1 antibodies, as indicated. The resulting immunocomplexes were analyzed by immunoblotting with anti-NIK antibodies. Where indicated, the cell extracts were immunoprecipitated with preimmune IgG (*IgG*) as a control. The expression of NIK and DSCR1 in the cell extracts was determined by Western blotting.

action between DSCR1 and NIK, we used several deletion constructs encoding DSCR1 fragments fused to GFP in similar co-immunoprecipitation assays. As shown in Fig. 3*A*, we found that NIK co-immunoprecipitated with the full-length DSCR1 protein as well as with the DSCR1 peptide fragments containing amino acids 30–197 and 90–197. Interestingly, NIK did not co-immunoprecipitate with a DSCR1 peptide fragment containing the N-terminal 90 amino acids (Fig. 3), suggesting that the DSCR1 domain critical for interacting with NIK is included within amino acid residues 90–197. Furthermore, when we examined whether wild type DSCR1 binds to the kinase-deficient NIK mutant, DSCR1 binds to wild type NIK but not to its kinase-dead mutant, such as NIK-KD or NIK-KK/AA (Fig. 3*B*).

NIK Phosphorylates DSCR1 in H19-7 Cells—Next, we examined whether DSCR1 is a substrate of NIK. We have previously shown that zinc induces the phosphorylation and activation of IKK in H19-7 cells (24). NIK is known to function as an upstream activator of the NF-κB signaling pathway that ultimately results in the activation of IKKα (15). Therefore, we first examined whether NIK is also phosphorylated and activated by zinc. H19-7 cells were either transfected with Myc-tagged NIK plasmid or mock-transfected and then stimulated with zinc plus the zinc ionophore, pyrithione. Lysates from the resulting transfected cells were subjected to immunoblotting using anti-phospho-NIK antibodies. As shown in Fig. 4*A*, treatment with zinc plus pyrithione induced the phosphorylation of endogenous NIK. Furthermore, the cells transfected with wild type NIK had much higher levels of phosphorylated NIK than the mock-transfected cells (Fig. 4*A*). To examine the effects of zinc treatment on NIK-associated DSCR1 phosphorylation, H19-7 cells were transfected with Myc-tagged NIK and then either untreated or treated with zinc plus pyrithione. Lysates from the resulting transfected cells were immunoprecipitated using anti-NIK antibodies, and these immunocomplexes were then used in *in vitro* kinase assays with recombinant GST-DSCR1 as the substrate. The results, shown in Fig. 4*B*, demonstrate that whereas DSCR1 was phosphorylated by anti-NIK immunocomplexes from untreated cells, the phos-

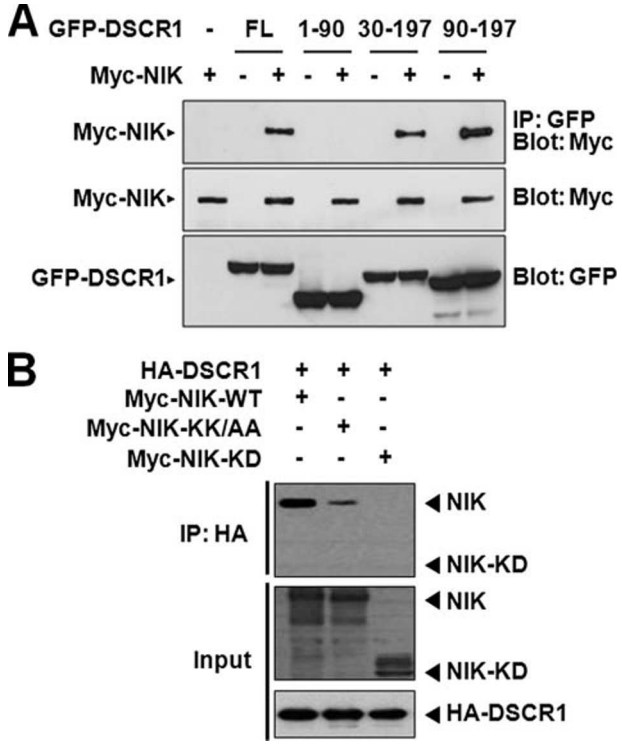

FIGURE 3. **NIK binds to the C-terminal domain of DSCR1.** *A,* HEK293 cells were transfected with Myc-tagged NIK alone or together with the various GFP-fused DSCR1 deletion mutants, as indicated. Lysates from the transfected cells were subjected to anti-GFP immunoprecipitation (*IP*) followed by anti-Myc immunoblotting. Total expression levels of the transfected proteins were assessed by immunoblotting with anti-GFP or anti-Myc antibodies, as indicated. *B,* cells were transfected with HA-tagged DSCR1 with Myc-tagged wild type NIK or its kinase-dead mutants, as indicated. Lysates from the transfected cells were subjected to anti-HA immunoprecipitation followed by anti-Myc immunoblotting. Total expression levels of the transfected proteins were assessed by immunoblotting with anti-Myc or anti-HA antibodies, as indicated.

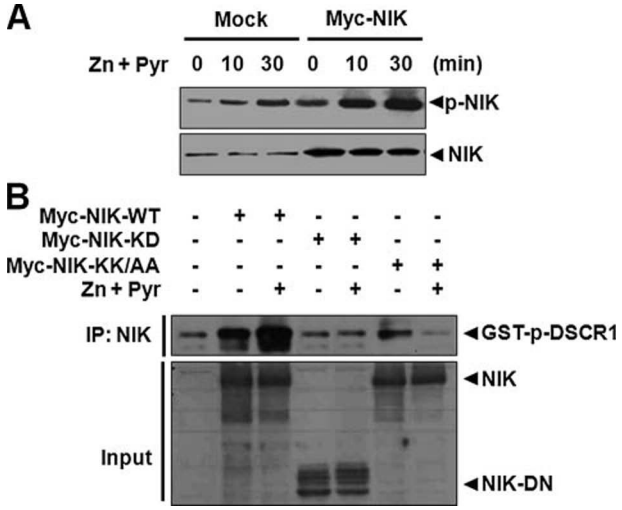

FIGURE 4. **NIK phosphorylates DSCR1 in H19-7 cells.** *A,* H19-7 cells were mock-transfected (*Mock*) or transiently transfected with 5 μg of Myc-tagged NIK. The cells were then treated with 10 μM zinc and pyrithione for the indicated times. Lysates from these cells were immunoblotted with either anti-phospho-NIK or anti-NIK antibodies, as indicated. *B,* cells were transfected with 5 μg Myc-tagged wild type NIK or a kinase-inactive NIK mutant (Myc-NIK-DN or Myc-NIK-KKAA). Twenty four hours later, the cells were either untreated or treated with 10 μM zinc and pyrithione for 30 min. Lysates from these cells were immunoprecipitated with anti-Myc antibodies followed by *in vitro* kinase assays using bacterially expressed GST-DSCR1 as a substrate. The kinase assay reaction products were resolved by 10% SDS-PAGE, and the levels of phosphorylated DSCR1 were visualized by autoradiography. The expression of NIK in cell lysates was analyzed by Western blotting with anti-NIK antibodies, as indicated.

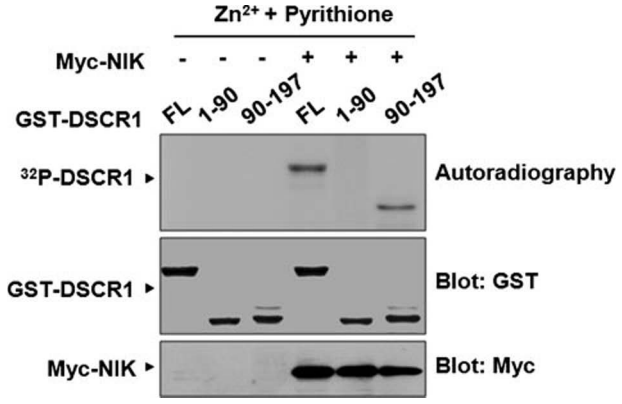

FIGURE 5. **NIK phosphorylates DSCR1 in its C-terminal region spanning amino acids 90–197.** GST-tagged constructs encoding full length (*FL*) (residues 1–197), amino acid residues 1–90, or amino acid residues 90–197 of DSCR1 were phosphorylated *in vitro* in the presence or absence of zinc-activated Myc-tagged NIK immunocomplexes expressed in H19-7 cells. The proteins were separated by 10% SDS-PAGE and visualized by autoradiography. Total expression of the GST-tagged DSCR1 peptides and Myc-NIK were verified by immunoblotting with anti-GST or anti-Myc antibodies, as indicated.

phorylation was significantly higher with anti-NIK immunocomplexes from cells treated with zinc plus pyrithione. Furthermore, this increase in DSCR1 phosphorylation was not observed in cells transfected with a kinase-inactive dominant-negative NIK mutant (Fig. 4*B*). These results demonstrate that wild type NIK specifically phosphorylates DSCR1, and the phosphorylation of DSCR1 is significantly induced by zinc treatment.

NIK Phosphorylates C-terminal Domain of DSCR1—To determine which domain(s) of DSCR1 are specifically phosphorylated by NIK, three bacterially expressed DSCR1 fragments fused with GST were purified and used as a substrate of NIK in *in vitro* kinase assay. As shown in Fig. 5, full-length DSCR1 and DSCR1 peptide fragment containing amino acid residues 90–197 could be phosphorylated by NIK following zinc plus pyrithione treatment. However, DSCR1 peptide fragment containing amino acid residues 1–90 could not be phosphorylated by NIK (Fig. 5). These data suggest that NIK specifically phosphorylates DSCR1 on a domain within amino acid residues 90–197.

The NIK-mediated Phosphorylation of DSCR1 Leads to an Increased Half-life and Reduced Proteasomal Degradation—Next, we examined the physiological consequence(s) of NIK-mediated DSCR1 phosphorylation. First, we examined whether this phosphorylation affects the half-life of DSCR1. Cells were transfected with HA-tagged DSCR1 alone or together with either wild type NIK or kinase-deficient mutants. The transfected cells were then incubated with cycloheximide for the indicated times. The levels of DSCR1 in these cells were measured by Western blot analysis using an anti-HA antibody. The cells transfected with DSCR1 and wild type NIK had ~2-fold more DSCR1 than the cells transfected with DSCR1 alone (Fig. 6, *A* and *B*). Interestingly, this increase in DSCR1 protein levels was not observed in the cells transfected with DSCR1 and the

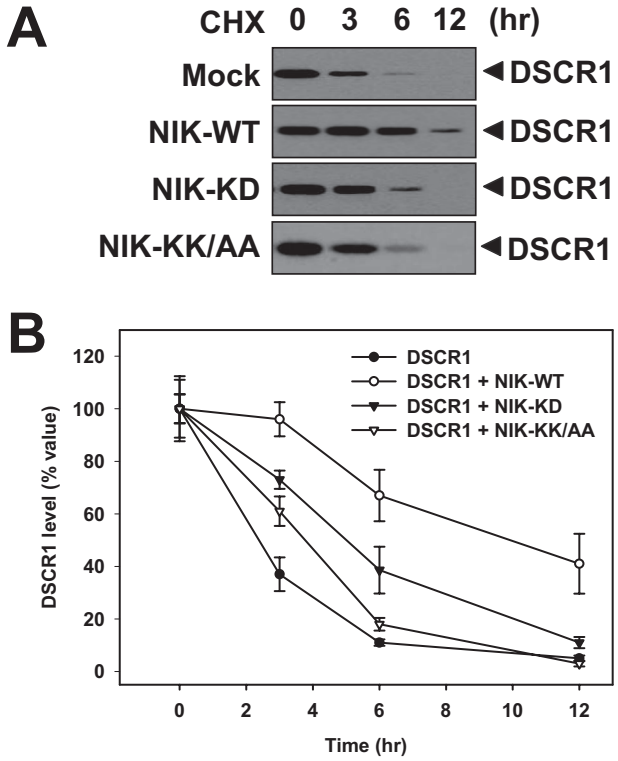

FIGURE 6. **NIK increases the half-life of DSCR1.** *A,* H19-7 cells were either mock-transfected (*Mock*) or transfected with Myc-tagged wild type NIK (*NIK-WT*) or kinase-deficient NIK mutants (*NIK-KD* or *NIK-KK/AA*), as indicated. Twenty four hours later, the cells were treated with 100 μM cycloheximide (*CHX*) for the indicated times and then harvested in PBS. The endogenous levels of soluble DSCR1 were determined by Western blot analysis with anti-DSCR1 antiserum. The results shown are representative of three independent experiments. *B,* relative levels of DSCR1 in the blots described in *A* were quantified and plotted ($n = 3$).

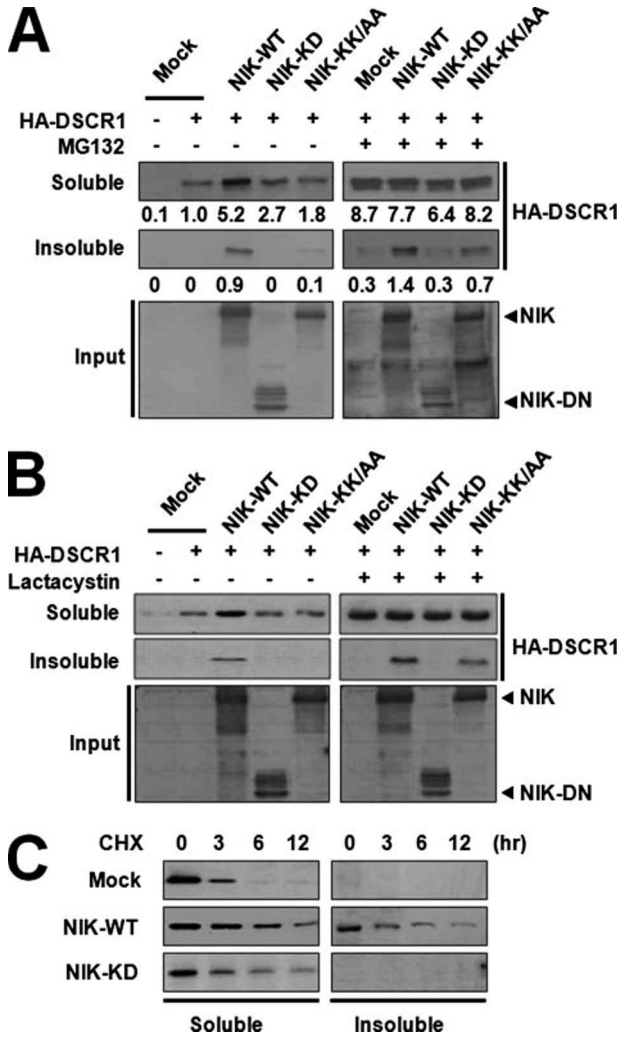

FIGURE 7. **NIK-mediated phosphorylation reduces DSCR1 degradation by the proteasomal pathway.** H19-7 cells were either mock-transfected (*Mock*) or transiently transfected with 3 μg of HA-tagged DSCR1 alone or together with either Myc-tagged wild type NIK or a kinase-inactive NIK mutant (*NIK-KD* or *NIK-KKAA*). Twenty four hours later, the cells were untreated or treated with 10 μM of MG132 (*A*) or clasto-lactacystin β-lactone (*Lactacystin*; *B*) for 6 h. The 1% Nonidet P-40-soluble and -insoluble fractions were separated. The presence of HA-tagged DSCR1 in each fraction was analyzed by immunoblotting with anti-HA antibodies. As a control, the levels of exogenous Myc-tagged NIK in the cell lysates were immunoanalyzed with anti-Myc antibodies, as indicated. The *numbers* at the bottom of the DSCR1 panels in *A* indicated quantitated values of fold induction measured using a densitometer. *C,* cells were either mock-transfected (*Mock*) or transfected with Myc-tagged wild type NIK (*NIK-WT*) or kinase-deficient NIK mutants (*NIK-KD* or *NIK-KK/AA*), as indicated. Twenty four hours later, the cells were treated with 100 μM cycloheximide (*CHX*) for the indicated times and then harvested in PBS. The 1% Nonidet P-40-soluble and -insoluble levels of DSCR1 were determined by Western blotting with anti-DSCR1 antiserum. The results shown are representative of three independent experiments.

kinase-dead NIK mutants (Fig. 6, *A* and *B*). These data suggest that the half-life of DSCR1 is increased by its NIK-mediated phosphorylation.

Next, we examined whether NIK alters the levels of 1% Nonidet P-40-soluble and -insoluble DSCR1. H19-7 cells were transfected with HA-tagged DSCR1 and/or Myc-tagged NIK. Lysates from the resulting transfected cells were blotted using anti-HA antibodies. As shown in Fig. 7, the levels of Nonidet P-40-soluble and -insoluble DSCR1 were increased in the cells co-transfected with wild type NIK. However, the levels of DSCR1 were not markedly changed in cells co-transfected with kinase-deficient NIK mutant, as compared with control cells transfected with DSCR1 alone (Fig. 7, *top, left panel*). These results indicate that the NIK-mediated phosphorylation of DSCR1 increases its stability in two different ways.

We have previously shown that the endogenous levels of DSCR1 are modulated by protein ubiquitination and proteasomal degradation in H19-7 cells (25). Based on the results described above, we examined whether NIK affects the proteasome-mediated degradation of DSCR1. We mock-transfected or transiently transfected cells with DSCR1 plus NIK and then treated the cells with the proteasomal inhibitor MG132. Lysates from these cells were then immunoblotted using anti-HA antibodies. As expected, MG132 treatment resulted in an increase in the levels of soluble DSCR1 and no apparent reduction in the level of insoluble DSCR1 in the absence of NIK (Fig. 7, *top right panel*). This finding supports the hypothesis that DSCR1 is constitutively degraded by proteasome. The increase in soluble DSCR1 levels was not altered by the presence of NIK or its kinase activity. Interestingly, MG132 treatment of cells transfected with wild type NIK resulted in the accumulation of insoluble DSCR1 relative to the mock-transfected control cells (Fig. 7*A*, *middle panel*). This result indicates that, in addition to the inhibitory effect on the proteasomal targeting, NIK also affects the stability of DSCR1 by altering its solubility. Similar results

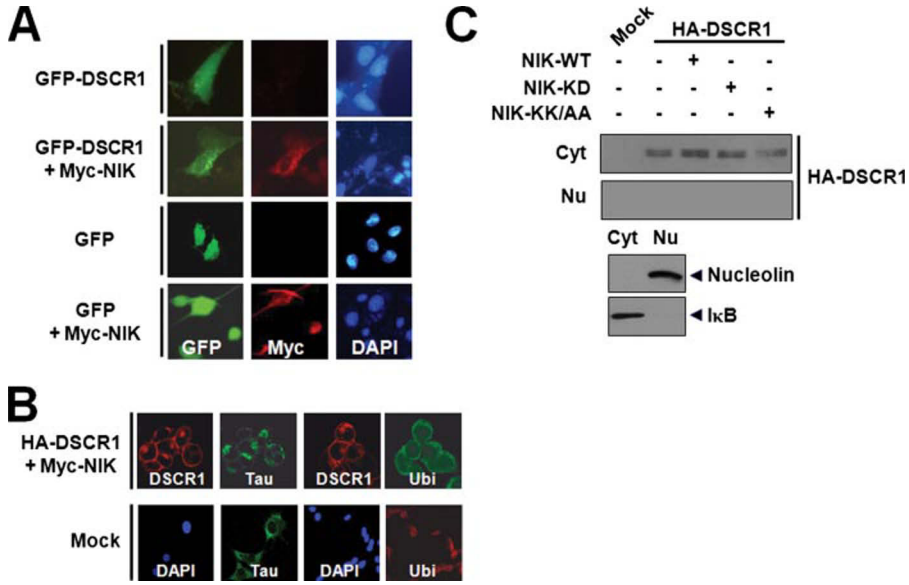

FIGURE 8. **NIK promotes the formation of cytosolic DSCR1 aggregates in H19-7 cells.** *A,* H19-7 cells were transfected with GFP or GFP-tagged DSCR1 alone or together with Myc-tagged NIK. Twenty four hours later, the cells were fixed, permeabilized, and labeled with anti-Myc antibodies and then stained with rhodamine-attached secondary antibodies and 4′,6-diamidino-2-phenylindole (*DAPI*). Immunostained preparations were examined by fluorescence microscopy. *B,* H19-7 cells were mock-transfected or transiently transfected with HA-tagged DSCR1 and Myc-tagged NIK. Twenty four hours later, the cells were immunolabeled with anti-HA, anti-ubiquitin (*Ubi*), or anti-Tau antibodies followed by staining with rhodamine- or fluorescein isothiocyanate-conjugated secondary antibodies. Immunostained preparations were examined via confocal microscopy. As a control, the distribution of Tau and ubiquitin in mock-transfected cells was shown, as indicated. *C,* cells were either mock-transfected (*Mock*) or transfected with 3 μg of HA-tagged DSCR1 alone or together with 3 μg of Myc-tagged wild type NIK or a kinase-inactive NIK mutant (*NIK-KD* or *NIK-KKAA*). Twenty four hours later, the cell lysates were fractionated into cytosolic (*Cyt*) and nuclear (*Nu*) fractions. The level of DSCR1 in each fraction was examined by Western blotting with anti-HA antibodies. The purity of each fraction was determined with antiserum specific for regional protein markers, such as nuclear nucleolin and cytosolic IκB protein.

were observed when another proteasomal inhibitor, clasto-lactacystin β-lactone, was used (Fig. 7*B*).

Next we tested whether NIK also affects the half-life of DSCR1 in 1% Nonidet P-40-insoluble fraction. As shown in Fig. 7*C*, the cells transfected with DSCR1 and wild type NIK had also greatly increased the stability of DSCR1 in Nonidet P-40-insoluble pellet fraction than the cells transfected with DSCR1 alone. Furthermore, this increase was not observed in the cells transfected with DSCR1 and the kinase-dead NIK mutants, which is the same manner to that in Nonidet P-40-soluble DSCR1 fraction (Fig. 7*C*). These data suggest that the stability of 1% Nonidet P-40-soluble and -insoluble DSCR1 is increased by NIK-mediated phosphorylation.

NIK Promotes the Formation of Cytosolic DSCR1 Aggregates—Next, we examined whether the NIK-mediated increase in the levels of insoluble DSCR1 leads to the formation of DSCR1 aggregates. H19-7 cells were either transfected with GFP, GFP-tagged DSCR1, or GFP-tagged DSCR1 and Myc-tagged NIK. GFP-mediated fluorescence was observed using a fluorescence microscope. As shown in Fig. 8*A*, cells transfected with GFP-DSCR1 alone displayed an even distribution of GFP signal in the cytosol as well as in the nucleus. In contrast, the cells transfected with GFP-DSCR1 and Myc-NIK displayed marked cytosolic DSCR1 aggregates (Fig. 8*A*). In addition, immunostaining of the cells using an anti-Tau antibody revealed that the DSCR1 aggregates contain a significant amount of Tau protein (Fig. 8*B*), which is also found in neurofibrillary tangle structure. Furthermore, immunostaining using anti-ubiquitin antibodies revealed the DSCR1 aggregates also contain ubiquitin (Fig. 8*B*). To further examine cytosolic DSCR1 inclusions, the cells were fractionated into cytosolic and nuclear fractions, and the presence of DSCR1 in each fraction was determined. The levels of DSCR1 in cytosolic fraction of cells co-transfected with wild type NIK was enhanced relative to that observed in the cells transfected with DSCR1 alone or DSCR1 plus a kinase-inactive NIK mutant (Fig. 8*C*). In addition, DSCR1 was not detected in the nuclear fraction of any cells examined (Fig. 8*C*). The purities of the prepared fractions were confirmed by Western blot analysis with antiserum against regional markers, such as nuclear nucleolin and cytosolic IκB protein (Fig. 8*C*). Together, these findings suggest that the NIK-mediated phosphorylation of DSCR1 inhibits its degradation, which ultimately results in its cytosolic aggregation.

The Formation of DSCR1 Aggregates Caused by NIK-mediated Phosphorylation Has No Effect on H19-7 Cell Viability—Next, we examined whether NIK-mediated phosphorylation of DSCR1 that ultimately leads to its cytosolic aggregation alters cell viability. H19-7 cells were transfected with HA-tagged DSCR1 and/or Myc-tagged wild type or kinase-deficient NIK mutant. Twenty four hours later, cell viability was measured by an MTT extraction method. As shown in Fig. 9*A*, the overexpression of DSCR1 induced cell death. A TUNEL assay revealed that this DSCR1-induced cell death is a result of apoptosis (Fig. 9*B*). In contrast, cells were transfected with DSCR1, and either wild type NIK or kinase-deficient mutants had no significant changes in viability, relative to control cells transfected with DSCR1 alone (Fig. 9*A*). Additional TUNEL assay demonstrated that DSCR1 phosphorylation and the cytotoxicity induced by its overexpression are not synergistic (Fig. 9*B*). These data suggest that the NIK-mediated increase in soluble and insoluble DSCR1 levels are not the cause of neuronal cell death associated with DSCR1 overexpression.

DISCUSSION

DSCR1 is known to attenuate the calcineurin-dependent signaling of NF-AT, thereby inhibiting cell proliferation and angiogenesis (8, 26). NF-AT has been shown to cooperate with NF-κB to up-regulate the expression of many inflammatory genes. For example, thrombin-mediated activation of endothelial cells involves interplay between NF-AT and NF-κB signaling pathways and their respective negative feedback inhibitors DSCR1 and IκB (26). Additionally, many reports have implicated calcineurin in the inflammatory NF-κB signaling path-

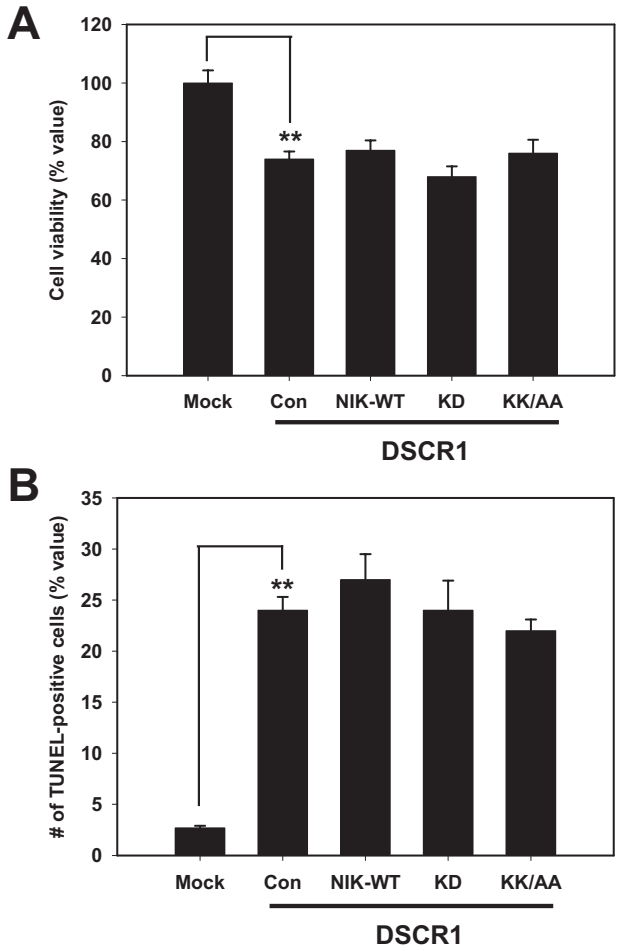

FIGURE 9. **The formation of cytosolic DSCR1 aggregates does not affect neuronal cell viability.** *A,* H19-7 cells were mock-transfected (*Mock*) or transiently transfected with 3 μg of HA-tagged DSCR1 alone or together with wild type Myc-tagged NIK (NIK-WT) or a kinase-deficient NIK mutant (NIK-DN or NIK-KA). Twenty four hours later, cell viability was measured with the MTT extraction assay. *B,* the number of TUNEL-positive apoptotic cells was measured by TUNEL assay (**, $p < 0.01$ vs control).

way. For example, calcineurin was shown to stimulate NF-κB activity by enhancing the inactivation and degradation of IκB (27, 28), and in T lymphocytes, protein kinase C and calcineurin have been shown synergistically to activate IκB kinase and NF-κB (29). Moreover, Biswas *et al.* (30) showed that NF-κB/Rel factor-bound IκBβ subunit forms a ternary complex with calcineurin *in vitro* and *in vivo*, and phosphorylated IκBβ is a substrate for calcineurin phosphatase. In neurons calcineurin plays a role maintaining and modulating basal NF-κB activity (31). Recently, DSCR1 was shown to inhibit the expression of genes involved in the inflammatory response and to attenuate NF-κB-mediated transcriptional activation by stabilizing its inhibitory protein, IκBα (32).

In this study, we showed that NIK, which functions in the alternative NF-κB signaling pathway, physically interacts with DSCR1 in mammalian neuronal cells. We also demonstrated that NIK can phosphorylate the C-terminal region of DSCR1, which ultimately leads to an increase in protein stability by attenuating the proteasome-mediated degradation of DSCR1. These results suggest that DSCR1 may participate or play a role in the inflammatory NF-κB signal transduction pathway.

The phosphorylation of DSCR1 or DSCR1 homologs was previously shown to affect the regulation of calcineurin. Specifically, the treatment of human U251 and HeLa cells with hydrogen peroxide and peroxynitrate results in the rapid hyperphosphorylation of DSCR1 (at the SPP motifs within the proline-rich region corresponding to amino acids 96–125), which ultimately results in the inhibition of calcineurin (33). Additionally, GSK-3 kinase has been shown to phosphorylate RCN1 at Ser-133, the DSCR1 homolog in *Caenorhabditis elegans*, which then goes on to regulate calcineurin signaling (34). Furthermore, MEK5 and BMK1 are shown to phosphorylate DSCR1 at Ser-112 (35). When phosphorylated, DSCR1 is dissociated from calcineurin and binds with 14-3-3, thereby relieving its inhibitory effect on calcineurin activity (35).

In this study, we found that the overexpression of DSCR1 in H19-7 cells results in neurotoxicity and its subsequent phosphorylation results in the formation of cytosolic aggregates. The aggregation of improperly folded peptides likely plays a key role in the pathogenesis of many neurodegenerative diseases (36, 37). Most DS patients develop phenotypes characteristic of the neurodegenerative Alzheimer disease, such as the deposition of amyloid-β and neurofibrillary tangles (38) and the severe loss of neuronal cells (39–41). It has been suggested that the chronic overexpression of genes located on chromosome 21 leads to the development of these Alzheimer disease phenotypes. Interestingly, DSCR1 has been shown to be overexpressed in the brains of Alzheimer disease patients (42, 43). Furthermore, the overexpression of DSCR1 decreases the phosphatase activity of calcineurin, which consequently causes the accumulation of hyperphosphorylated Tau protein (a major component of tangle) and cytoskeletal changes in the hippocampus, two events similar to those observed during the development of Alzheimer disease (44–46). These findings suggest that aberrant expression of DSCR1 may play a role in AD pathogenesis. The data presented in this study indicate that, whereas the aberrant expression of DSCR1 induces cytotoxicity in neuronal cells, the NIK-mediated phosphorylation of DSCR1 is less prone digestion, which ultimately leads to the formation of Tau-like aggregates.

Our current data demonstrate that DSCR1 aggregate formation does not exaggerate the neurotoxic effect associated with its accumulation. This finding supports the hypothesis that the formation of an intracytoplasmic DSCR1 aggresome is not itself toxic and may not play a role in the establishment of the pathological degenerative changes associated with Down syndrome. Recently, it has been hypothesized that amyloid deposits themselves are not the actual causes of neurodegeneration but rather the oligomeric intermediates that eventually lead to the formation these deposits are the cause(s) (37, 47). It is believed that the formation of amyloid deposits is a simple end product of a detoxification process that is designed to protect the cell from such toxic intermediates. This hypothesis is supported by recent studies demonstrating that prefibrillar intermediates (protofibrils) and not mature amyloid fibrils are the key toxic species in Alzheimer disease, Parkinson disease, and Huntington disease. The toxicity of protofibrils in Alzheimer disease is illustrated in the finding that small oligomers of Aβ potently inhibit long term potentiation of the hippocampus *in vivo*,

whereas fibrillar and monomeric forms have no effect (48). These results are further supported by another independent study that demonstrated that when two proteins were incubated under conditions in which amyloid fibrils were formed, only the prefibrillar intermediates and not the mature fibrils caused cytotoxicity (49). Therefore, further experiments will be required, and it will be interesting to check whether these DSCR1 aggregates contain misfolded protein components and consequently possess the amyloid or prefibrillar structure through *in vivo* and *in vitro* staining with Congo red or/and thioflavin.

In summary, our study shows that NIK interacts with and phosphorylates DSCR1. Although the overexpression of DSCR1 decreases the viability of H19-7 cells, the NIK-mediated phosphorylation of DSCR1 leads to the formation of its aggregates, which do not to have an effect on cell viability. Further studies are required to determine whether and how DSCR1 regulates the NIK activity and subsequently the alternative NF-κB signaling pathway. The results of such studies would provide us with a greater understanding of the functional role of DSCR1 in NIK-mediated activation of the NF-κB signaling pathway.

Acknowledgments—We are deeply grateful to S. de la Luna, B. A. Rothermel, and T. H. Lee for generously providing plasmids.

REFERENCES

1. Epstein, C. J. (1995) *Prog. Clin. Biol. Res.* **393,** 241–246
2. Toyoda, A., Noguchi, H., Taylor, T. D., Ito, T., Pletcher, M. T., Sakaki, Y., Reeves, R. H., and Hattori, M. (2002) *Genome Res.* **12,** 1323–1332
3. Antonarakis, S. E., Lyle, R., Dermitzakis, E. T., Reymond, A., and Deutsch, S. (2004) *Nat. Rev. Genet.* **5,** 725–738
4. Roizen, N. J., and Patterson, D. (2003) *Lancet* **361,** 1281–1289
5. Fuentes, J. J., Pritchard, M. A., and Estivill, X. (1997) *Genomics* **44,** 358–361
6. Pfister, S. C., Machado-Santelli, G. M., Han, S. W., and Henrique-Silva, F. (2002) *BMC Cell Biol.* **3,** 24
7. Fuentes, J. J., Pritchard, M. A., Planas, A. M., Bosch, A., Ferrer, I., and Estivill, X. (1995) *Hum. Mol. Genet.* **4,** 1935–1944
8. Fuentes, J. J., Genesca, L., Kingsbury, T. J., Cunningham, K. W., Perez-Riba, M., Estivill, X., and de la Luna, S. (2000) *Hum. Mol. Genet.* **9,** 1681–1690
9. Rothermel, B., Vega, R. B., Yang, J., Wu, H., Bassel-Duby, R., and Williams, R. S. (2000) *J. Biol. Chem.* **275,** 8719–8725
10. Vega, R. B., Rothermel, B. A., Weinheimer, C. J., Kovacs, A., Naseem, R. H., Bassel-Duby, R., Williams, R. S., and Olson, E. N. (2003) *Proc. Natl. Acad. Sci. U. S. A.* **100,** 669–674
11. Harris, C. D., Ermak, G., and Davies, K. J. (2005) *Cell. Mol. Life Sci.* **62,** 2477–2486
12. Hesser, B. A., Liang, X. H., Camenisch, G., Yang, S., Lewin, D. A., Scheller, R., Ferrara, N., and Gerber, H. P. (2004) *Blood* **104,** 149–158
13. Ryeom, S., Greenwald, R. J., Sharpe, A. H., and Mckeon, F. (2003) *Nat. Immunol.* **4,** 874–881
14. Yao, Y. G., and Duh, E. J. (2004) *Biochem. Biophys. Res. Commun.* **321,** 648–656
15. Ling, L., Cao, Z., and Goeddel, D. V. (1998) *Proc. Natl. Acad. Sci. U. S. A.* **95,** 3792–3797
16. Woronicz, J. D., Gao, X., Cao, Z., Rothe, M., and Goeddel, D. V. (1997) *Science* **278,** 866–869
17. Dejardin, E. (2006) *Biochem. Pharmacol.* **72,** 1161–1179
18. Yin, L., Wu, L., Wesche, H., Arthur, C. D., White, J. M., Goeddel, D. V., and Schreiber, R. D. (2001) *Science* **291,** 2162–2165
19. Birbach, A., Bailey, S. T., Ghosh, S., and Schmid, J. A. (2004) *J. Cell Sci.* **117,** 3615–3624
20. Crabtree, G. R. (1999) *Cell* **96,** 611–614
21. Zhu, J., and McKeon, F. (2000) *Cell. Mol. Life Sci.* **57,** 411–420
22. Luo, C., Shaw, K. T. Y., Raghavan, A., Aramburu, J., Garcia-Cozar, F., Perrino, B. A., Hogan, P. G., and Rao, A. (1996) *Proc. Natl. Acad. Sci. U. S. A.* **93,** 8907–8912
23. Cho, Y. J., Abe, M., Kim, S. Y., and Sato, Y. (2005) *Arch. Biochem. Biophys.* **439,** 121–128
24. Min, Y. K., Park, J. H., Chong, S. A., Kim, Y. S., Ahn, Y. S., Seo, J. T., Bae, Y. S., and Chung, K. C. (2003) *J. Neurosci. Res.* **71,** 689–700
25. Lee, E. J., Lee, J. Y., Seo, S. R., and Chung, K. C. (2007) *Mol. Cell. Neurosci.* **35,** 585–595
26. Minami, T., Horiuchi, K., Miura, M., Abid, M. R., Takabe, W., Noguchi, N., Kohro, T., Ge, X., Aburatani, H., Hamakubo, T., Kodama, T., and Aird, W. C. (2004) *J. Biol. Chem.* **279,** 50537–50554
27. Frantz, B., Nordby, E. C., Bren, G., Steffan, N., Paya, C. V., Kincaid, R. L., Tocci, M. J., O'Keefe, S. J., and O'Neill, E. A. (1994) *EMBO J.* **13,** 861–870
28. Steffan, N. M., Bren, G. D., Frantz, B., Tocci, M. J., O'Neill, E. A., and Paya, C. V. (1995) *J. Immunol.* **155,** 4685–4691
29. Trushin, S. A., Pennington, K. N., Algeciras-Schimnich, A., and Paya, C. V. (1999) *J. Biol. Chem.* **274,** 22923–22931
30. Biswas, G., Anandatheerthavarada, H. K., Zaidi, M., and Avadhani, N. G. (2003) *J. Cell Biol.* **161,** 507–519
31. Lilienbaum, A., and Israël, A. (2003) *Mol. Cell. Biol.* **23,** 2680–2698
32. Kim, Y. S., Cho, K. O., Lee, H. J., Kim, S. Y., Sato, Y., and Cho, Y. J. (2006) *J. Biol. Chem.* **281,** 39051–39061
33. Lin, H. Y., Michtalik, H. J., Zhang, S., Andersen, T. T., Van Riper, D. A., Davies, K. K., Ermak, G., Petti, L. M., Nachod, S., Narayan, A. V., Bhatt, N., and Crawford, D. R. (2003) *Free Radic. Biol. Med.* **35,** 528–539
34. Hilioti, Z., Gallagher, D. A., Low-Nam, S. T., Ramaswamy, P., Gajer, P., Kingsbury, T. J., Birchwood, C. J., Levchenko, A., and Cunningham, K. W. (2004) *Genes Dev.* **18,** 35–47
35. Abbasi, S., Lee, J. D., Su, B., Chen, X., Alcon, J. L., Yang, J., Kellems, R. E., and Xia, Y. (2006) *J. Biol. Chem.* **281,** 7717–7726
36. Ross, C. A., and Poirier, M. A. (2005) *Nat. Rev. Mol. Cell Biol.* **26,** 891–898
37. Ross, C. A., and Poirier, M. A. (2004) *Nat. Med.* **10,** S10–S17
38. Coyle, J. T., Oster-Grunite, M. L., and Gearhard, J. D. (1986) *Brain Res. Bull.* **16,** 773–787
39. Mann, D. M., Yates, P. O., Marcyniuk, B., and Ravindra, C. R. (1987) *J. Neurol. Sci.* **80,** 79–89
40. Tanzi, R. E. (1996) *Nat. Med.* **2,** 31–32
41. Wisniewski, K. E., Laure-Kamionowska, M., and Wisniewski, H. M. (1984) *N. Engl. J. Med.* **311,** 1187–1188
42. Cook, C. N., Hejna, M. J., Magnuson, D. J., and Lee, J. M. (2005) *J. Alzheimer's Dis.* **8,** 63–73
43. Ermak, G., Margan, T. E., and Davies, K. J. (2001) *J. Biol. Chem.* **276,** 38787–38794
44. Davies, K. J., Harris, C. D., and Ermak, G. (2001) *Biofactors* **15,** 91–93
45. Suzuki, K., Miura, T., and Takeuchi, H. (2001) *Biochem. Biophys. Res. Commun.* **285,** 991–996
46. Lukiw, W. J., and Bazan, N. G. (2000) *Neurochem. Res.* **25,** 1173–1184
47. Lansbury, P. T., and Lashuel, H. A. (2006) *Nature* **443,** 774–779
48. Walsh, D. M., Klyubin, I., Fadeeva, J. V., Cullen, W. K., Anwyl, R., Wolfe, M. S., Rowan, M. J., and Selkoe, D. J. (2002) *Nature* **416,** 535–539
49. Bucciantini, M., Giannoni, E., Chiti, F., Baroni, F., Formigli, L., Zurdo, J., Taddei, N., Ramponi, G., Dobson, C. M., and Stefani, M. (2002) *Nature* **416,** 507–511